COMPUTATION OF STEADY FLOW IN A TURBOMACHINERY STAGE BY A THIRD-ORDER ACCURATE HIGH-RESOLUTION SCHEME

Jixian Yao* Shanhong Ji† Feng Liu‡
Department of Mechanical and Aerospace Engineering
University of California, Irvine, CA92697

Ian K. Jennions§
ABB Power Generation, Baden, Switzerland

Abstract

This paper extends a third-order accurate ENO scheme with implicit LU-SGS time-stepping to calculate flow in a multiple blade row environment. The flow is considered steady relative to each blade row individually and the rows communicate via inter-blade-row mixing planes. The inter-blade-row mixing plane introduces circumferential averaging of flow properties but preserves spanwise variations. The flows through a turbine stage and a compressor stage are calculated. Comparisons between numerical results and measurements are provided.

1 Introduction

As the performance of turbomachines steadily improves, designers become more and more interested in flow predictions of blade rows in a multistage environment, rather than traditional single-blade row calculations.

In the calculation of flow in an isolated blade row, proper inflow and outflow conditions must be specified before the calculation. These conditions are usually taken from a multistage through-flow calculation, which, however, may not be consistent with the results of full three-dimensional Navier-Stokes calculations. In an actual multiple blade-row environment, only the flow conditions at the inlet and outlet of the whole machine are known, whereas the flow conditions, such as the total pressure, total temperature and flow directions in between the blade rows are unknown a priori and should be determined jointly by the flow conditions in the blade rows upstream and downstream. Strictly speaking, an unsteady simulation must be carried out to predict the actual physical flow. However, such unsteady calculations of multiple blade-row flows are still not practical for use in routine design work at this time due to computational time limit.

Following Denton[1], we solve the steady flow in each blade row and introduce inter-blade-row mixing planes to take into account of the flow communications between the blade rows. Computation of each blade row is carried out individually. However, the inter-blade-row boundary conditions are communicated between the blade rows These mixing planes introduce circumferential averaging of conservative flow variables, but preserve general radial variations. through the inter-blade-row mixing planes at each time step. No inter-blade-row boundary conditions need be specified. Instead, they come out as solutions of the complete multi-blade row calculations when the computations converge.

Compared to an unsteady calculation, the steady method with inter-blade-row mixing planes takes less time and effort. It provides an expedient tool for prediction of the overall performance of a multistage machine.

In this paper, a flow solver which employs a third order essentially non-oscillatory scheme (ENO3) and symmetric lower-upper Gause-Seidel implicit scheme (LU-SGS) is developed to calculate the steady flow in multiple blade rows by using the mixing plane approach. Solutions are presented for a turbine stage and a compressor stage and compared with experimental data.

2 Equations and Schemes

The time-averaged Navier-Stokes equations in cylindrical coordinates (θ, r, z) can be written in the generalized curvilinear coordinates (ξ, η, ζ) fixed to a blade row as follows:

*Postdoctoral Fellow, Member AIAA
†Research Assistant, Student Member AIAA
‡Associate Professor, Member AIAA
§Manager, Member AIAA

$$\frac{\partial Q}{\partial t}+\frac{\partial E}{\partial \xi}+\frac{\partial F}{\partial \eta}+\frac{\partial G}{\partial \zeta}=K+\frac{\partial E_v}{\partial \xi}+\frac{\partial F_v}{\partial \eta}+\frac{\partial G_v}{\partial \zeta} \qquad (1)$$

where

$$Q = J^{-1}\begin{bmatrix} r\rho \\ r\rho u \\ r\rho v \\ r\rho w \\ re \end{bmatrix}$$

$$E,F,G = J^{-1}\begin{bmatrix} r\rho\Theta_k \\ r\rho u\Theta_k + rpk_\theta/r \\ r\rho v\Theta_k + rpk_r \\ r\rho w\Theta_k + rpk_z \\ r\Theta_k(e+p)+\omega r^2 pk_\theta/r \end{bmatrix}$$

$$K = J^{-1}\begin{bmatrix} 0 \\ -\rho uv+\tau_{\theta r} \\ \rho u^2 + p - \tau_{\theta\theta} \\ 0 \\ 0 \end{bmatrix}$$

$$E_v,F_v,G_v = J^{-1}\begin{bmatrix} 0 \\ \tau_{\theta\theta}k_\theta + r\tau_{\theta r}k_r + r\tau_{\theta z}k_z \\ \tau_{r\theta}k_\theta + r\tau_{rr}k_r + r\tau_{rz}k_z \\ \tau_{z\theta}k_\theta + r\tau_{zr}k_r + r\tau_{zz}k_z \\ T_\theta k_\theta + rT_r k_r + rT_z k_z \end{bmatrix}$$

$$k=\xi,\eta,\zeta \text{ for } E_v, F_v, \text{ and } G_v \text{ respectively}$$

$$\Theta_k = (u-\omega r)k_\theta/r + vk_r + wk_z$$

$$T_\theta = \tau_{\theta\theta}u + \tau_{\theta r}v + \tau_{\theta z}w - q_\theta$$

$$T_r = \tau_{r\theta}u + \tau_{rr}v + \tau_{rz}w - q_r$$

$$T_z = \tau_{z\theta}u + \tau_{zr}v + \tau_{zz}w - q_z$$

$$\tau_{\theta\theta} = \frac{2}{3}(\mu+\mu_t)[2\frac{\partial u}{r\partial\theta} - \frac{\partial v}{\partial r} - \frac{\partial w}{\partial z} + 2\frac{v}{r}]$$

$$\tau_{rr} = \frac{2}{3}(\mu+\mu_t)[2\frac{\partial v}{\partial r} - \frac{\partial u}{r\partial\theta} - \frac{\partial w}{\partial z} - \frac{v}{r}]$$

$$\tau_{zz} = \frac{2}{3}(\mu+\mu_t)[2\frac{\partial w}{\partial z} - \frac{\partial u}{r\partial\theta} - \frac{\partial v}{\partial r} - \frac{v}{r}]$$

$$\tau_{\theta r} = \tau_{r\theta} = (\mu+\mu_t)[\frac{\partial u}{\partial r} + \frac{\partial v}{r\partial\theta} - \frac{u}{r}]$$

$$\tau_{rz} = \tau_{zr} = (\mu+\mu_t)[\frac{\partial v}{\partial z} + \frac{\partial w}{\partial r}]$$

$$\tau_{\theta z} = \tau_{z\theta} = (\mu+\mu_t)[\frac{\partial w}{r\partial\theta} + \frac{\partial u}{\partial z}]$$

$$q_\theta = -Cp(\frac{\mu}{\mathrm{Pr}} + \frac{\mu_t}{\mathrm{Pr_t}}\frac{\partial T}{r\partial\theta})$$

$$q_r = -Cp(\frac{\mu}{\mathrm{Pr}} + \frac{\mu_t}{\mathrm{Pr_t}}\frac{\partial T}{\partial r})$$

$$q_z = -Cp(\frac{\mu}{\mathrm{Pr}} + \frac{\mu_t}{\mathrm{Pr_t}}\frac{\partial T}{\partial z})$$

ρ is the density; u, v, and w are the absolute components of velocity in (θ, r, z) directions respectively; e is the total internal energy; ω is angular velocity; pressure $p=(\gamma-1)\big[e-\rho(u^2+v^2+w^2)/2\big]$, γ is the specific heat ratio. J is the metric Jacobian. τ and q are the shear stress tensor and heat flux vector respectively. Pr and $\mathrm{Pr_t}$ are the molecular and turbulent Prandtl number. Cp is the specific heat of constant pressure. μ and μ_t are the molecular and turbulent eddy viscosity, which are evaluated by Sutherland's formula and Baldwin-Lomax algebraic turbulence model[2].

An ENO scheme proposed by Yang[3] is employed for the convection terms. The original scheme by Yang is third-order accurate both in time and space. For steady calculation in this paper, we reduce the accuracy in time to first-order accuracy while keeping the third-order accuracy in space. The central difference is used for the viscous terms. The reduced scheme is described below.

For the convection term in ξ direction, the space discretization is as follows:

$$\frac{\partial E}{\partial \xi} = \hat{A}^+\Delta_- E_i^M + \hat{A}^-\Delta_+ E_i^M$$

where the modified vector is

$$E_i^M = E_i + C_i + D_i$$

$$C_i = \mathrm{minmod}(\tilde{C}_{i-\frac{1}{2}}, \tilde{C}_{i+\frac{1}{2}})$$

$$\tilde{C}_{i+\frac{1}{2}} = \mathrm{sgn}A_{i+\frac{1}{2}}\Delta_{i+\frac{1}{2}}E/2$$

$$D_i = \begin{cases} \bar{\mathrm{m}}(\Delta_-\tilde{D}_{i-\frac{1}{2}}, \Delta_+\tilde{D}_{i-\frac{1}{2}}) & \text{if } \left|\Delta_{i-\frac{1}{2}}Q\right| \le \left|\Delta_{i+\frac{1}{2}}Q\right| \\ \bar{\mathrm{m}}(\Delta_-\hat{D}_{i+\frac{1}{2}}, \Delta_+\hat{D}_{i+\frac{1}{2}}) & \end{cases}$$

$$\tilde{D}_{i+\frac{1}{2}} = \mathrm{sgn}A_{i+\frac{1}{2}}\Delta_{i+\frac{1}{2}}E/3$$

$$\hat{D}_{i+\frac{1}{2}} = -\mathrm{sgn}A_{i+\frac{1}{2}}\Delta_{i+\frac{1}{2}}E/6$$

A is the coefficient Jacobian in ξ direction, and

$$\mathrm{sgn}A = R\,\mathrm{diag}\{\mathrm{sgn}(a_l)\}\,L$$

$$\hat{A}^{\pm} = R\,\mathrm{diag}\{\hat{a}_l^{\pm}\}\,L$$

$$\hat{a}_l^{\pm} = (1 \pm \mathrm{sgn}a_l)/2$$

where L and R are the left and right eigen matrices respectively, a_l is the eigen values of A, $l = 1 \sim 5$.

$$\bar{\mathrm{m}}(a,b) = \begin{cases} a & \text{if } |a| \le |b| \\ b & \end{cases}$$

$$\mathrm{minmod}(a,b) = \begin{cases} s\,\min(|a|,|b|) & \text{if } \mathrm{sgn}a = \mathrm{sgn}b = s \\ 0 & \end{cases}$$

also, Δ_- and Δ_+ refer to backward and forward difference, and Δ refers central difference.

Similar expressions can be written for η and ζ directions.

3 LU-SGS Implicit Algorithm

The Lower-Upper implicit algorithm was originally proposed by Jameson and Turkel[4]. Yoon and Jameson[5] incorporate a special splitting method which eliminates the use of block matrix inversion in the implicit time stepping. This method is unconditionally stable in a three dimensional system.

The implicit scheme of Eq.(1) can be written in delta form:

$$\begin{aligned}&[\frac{I}{\Delta t}+(\Delta_- A^+ + \Delta_- B^+ + \Delta_- C^+)+ \\ &\qquad (\Delta_+ A^- + \Delta_+ B^- + \Delta_+ C^-)]\delta Q = R\end{aligned} \tag{2}$$

where R is the right hand side explicit part evaluated by the above techniques. A, B, C are the coefficient Jacobians in ξ, η, ζ directions, and

$$A^{\pm} = (A \pm r_A I)/2$$

$$B^{\pm} = (B \pm r_B I)/2$$

$$C^{\pm} = (C \pm r_C I)/2$$

r_A, r_B, r_C are the spectral radii of A, B, C. The LU decomposition of Eq.(2) is:

$$L\, D^{-1}\, U\, \delta Q = R$$

where

$$L = r_{ABC} I - A^+_{i-1} - B^+_{j-1} - C^+_{k-1}$$
$$D = r_{ABC} I$$
$$U = r_{ABC} I + A^-_{i+1} + B^-_{j+1} + C^-_{k+1}$$

$$r_{ABC} = \frac{1}{\Delta t} + r_A + r_B + r_C$$

The solving procedure is

L-operator:

$$\delta Q^* = (R + A^+_{i-1}\delta Q^*_{i-1} + B^+_{j-1}\delta Q^*_{j-1} + C^+_{k-1}\delta Q^*_{k-1}) / r_{ABC}$$

U-operator:

$$\delta Q = \delta Q^* - (A^+_{i+1}\delta Q^*_{i+1} + B^+_{j+1}\delta Q^*_{j+1} + C^+_{k+1}\delta Q^*_{k+1}) / r_{ABC}$$

Update:

$$Q^{n+1} = Q^n + \delta Q$$

4 Boundary Conditions and Mixing Model

Based on characteristic analysis, we fix the absolute total pressure, total temperature, tangential velocity, and radial velocity at the inflow boundary. The hub or tip back pressure is fixed for outflow boundary and the radial equilibrium equation is used to get the back pressure distribution in radial direction.

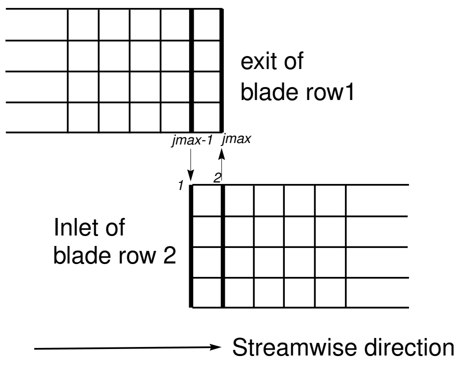

Figure 1: Overlapped grid of a mixing plane

We essentially follow Denton's approach. However, to facilitate the communication between blade rows, we use a "mixing plane" which consists of two overlapped grid planes as shown in Figure 1. The grid lines on these overlapped planes are matched in the radial direction but may mismatch in the circumferential direction. A simple mixing model is used for the current calculation, all the flow variables are area-averaged along the circumferential direction by the following equation, but the variations along the spanwise direction are retained.

$$\overline{Q} = \frac{\Sigma Q ds}{\Sigma ds}$$

where Q is one of $\rho, \rho u, \rho v, \rho w, e$.

As shown in Figure 1, the upstream blade row is calculated first, then the averaged flow properties from the second station from the exit (station jmax-1) are transferred to the first station (station 1) of the downstream blade row; Secondly, the downstream blade row is calculated, then the averaged flow properties from the second station (station 2) is transferred to the exit (station jmax) of the upstream blade row.

5 Results and Discussion

5.1 Flow through a turbine stage

The turbine stage we calculated is provided within the framework of ERCOFTAC[6], which is becoming a standard test case for computational methods. It has 36 vanes and 41 blades. Tip radius is 0.3m, hub radius is 0.245m, and rotational speed is 3500rpm. The computational grid consists of $37 \times 49 \times 130$ grid points for each blade row. Cross-sections of the grid in the blade-to-blade plane and the hub-tip plane are shown in Figure 2. The current calculation does not include the tip clearance.

The flow through the rotor is calculated both as a single rotor and as a stage consisting the turbine nozzle and the rotor.

The inlet and exit boundary conditions for the stage are taken from reference[7]. Figures 3, 4 and 5 show the computed circumferentially averaged relative total pressure, relative total temperature and relative flow angle distributions along the blade span at 8.8mm downstream the rotor trailing edge. The single rotor calculation is done by specifying the same rotor inlet total pressure, total temperature and flow angle distribution based on a through flow calculation as in reference[7].

In the stage calculation, such conditions from the through flow calculation are not needed since the iteration between the turbine nozzle and rotor calculation across the mixing plane produces the complete flow conditions at the rotor inlet. Reference[7] gave a detailed discussion on the flow features through this turbine rotor. The stagnation pressure peaks in the experimental data shown in Figure 3 are due to end-wall secondary flow vortices. It can be seen that the stage calculation predicts the hub secondary flow feature better than the single rotor calculation. However, both the single rotor and stage calculation seem to under-predict the loss peaks near the casing.

Figures 3, 4 and 5 show that the stage calculation provide better overall agreement with the experimental data than the single rotor calculation.

5.2 Flow through a compressor stage

Our second test case is a research compressor stage designed and tested by the Chinese Gas Turbine Establishment[8]. It has 28 rotor blades, 40 stator vanes. Rotor aspect ratio is 1.8, stator aspect ratio is 1.85. The hub-tip ratio is 0.5 for rotor and 0.6 for stator. Rotor tip radius is 0.3m. The rotor rpm is 13687. Figure 6 shows the computational grid with $41 \times 41 \times 93$ grid points for each blade row. Again, no tip clearance is modeled.

Comparisons of spanwise variations of mass averaged performance parameters at the mixing plane are shown in Figures 7, 8, and 9 for the case with a total pressure rise of 1.59 across the stage.

Figure 9 indicates that the computation overpredicts the turning angle across the rotor near the hub compared to the experimental data. This means that the root section of the rotor is over loaded resulting in a higher total pressure and temperature rise near the hub as shown in Figures 7 and 8. The computed results, however, do follow the overall trends of the experimental measurements in all of the three figures.

The overall performance of the whole stage is also calculated for this case. The back pressure is increased to reduce the mass flow rate. All other boundary conditions remain the same. Four operation points are calculated. As shown in Figure 10, both the predicted total pressure ratio line and the efficiency line agree reasonably well with the experiments. But the total pressure ratio is predicted higher near choke and the adiabatic efficiency is predicted higher near stall.

6 Concluding Remarks

A Navier-Stokes flow solver for calculating three-dimensional viscous flow in a turbomachinery stage via the use of an inter-blade-row mixing model is presented. This method eliminates the necessity of specifying inter-blade-row boundary conditions. The code is used to calculate the flow through a turbine stage and a compressor stage.

The computational results show general agreement with experimental data. Comparison of the single blade row calculation and the stage calculation for the turbine case indicates improved prediction of the flow over the single blade row approach.

Acknowledgement

Support for this research was provided by the National Science Foundation under grant CTS-9410800 and by ABB Power Generation Limited, Baden, Switzerland

References

[1] J. D. Denton, "The Calculation of Three Dimensional Viscous Flow Through Multistage Turbomachines", Trans. ASME, J. of Turbomachinery, Vol.114, 1992

[2] B. S. Baldwin and H. Lomax, "Thin Layer Approximation and Algebraic Model for Separated Turbulent Flows", AIAA P. 78-257

[3] J. Y. Yang, "Third Order Nonoscillatory Schemes for the Euler Equations", AIAA J. Vol.29, No.10, 1991

[4] A. Jameson and E. Turkel, "Implicit schemes and LU Decompositions", Math. of Comp., Vol.37, No.156, 1981, pp385-397

[5] S. Yoon and A. Jameson, "Lower-Upper Symmetric Gause-Seidel Method for the Euler and Navier-Stokes Equations", AIAA J. Vol.26, No.9, 1988

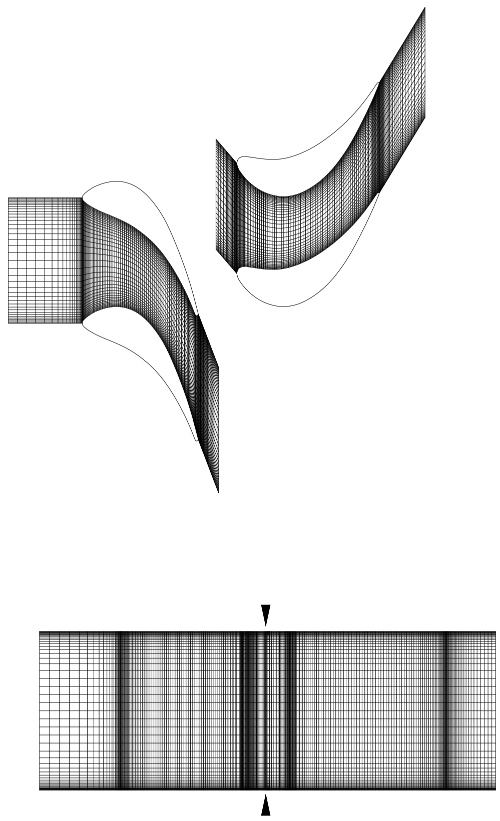

Figure 2: The computational grid of Aachen Stage

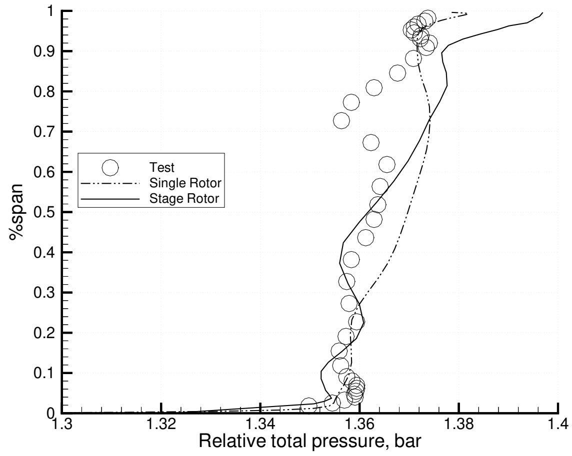

Figure 3: The spanwise total pressure, 8.8mm downstream trailing edge

[6] ERCOFTAC Test Case 6, 1.5 Stage Axial Flow Turbine, ERCOFTAC 1995

[7] R. Emunds, I. K. Jennions, D. Bohn and J. Gier, "The Computation of Adjacent Blade-Row Effects in a 1.5 Stage Axial Flow Turbine", ASME 97-GT-81, 1997

[8] The Design and Experiment Reports of A Turbofan Stage, GTE-95-SJ302, Gas Turbine Establishment, SiChuan, China, 1995

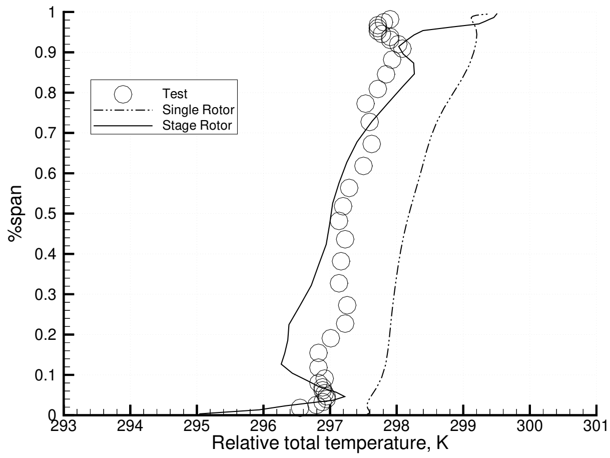

Figure 4: The spanwise total temperature, 8.8mm downstream trailing edge

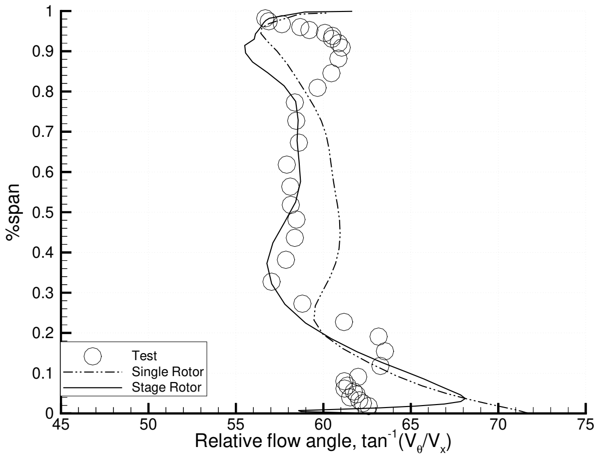

Figure 5: The spanwise flow angle, 8.8mm downstream trailing edge

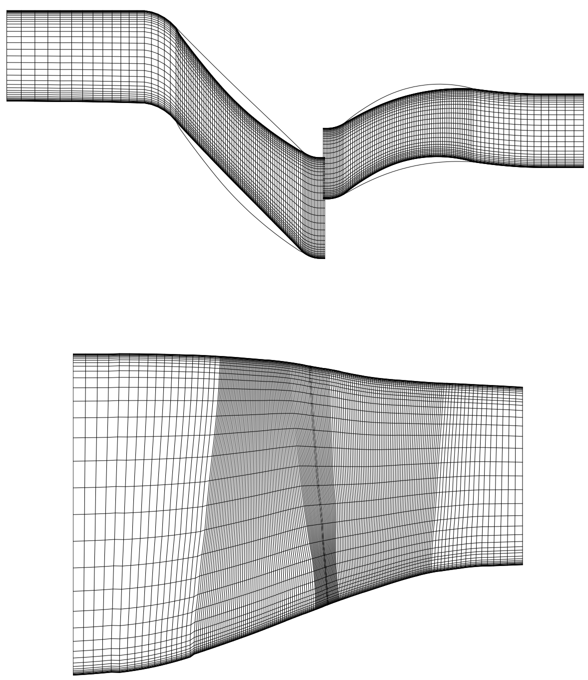

Figure 6: The computational grid of the one-stage compressor

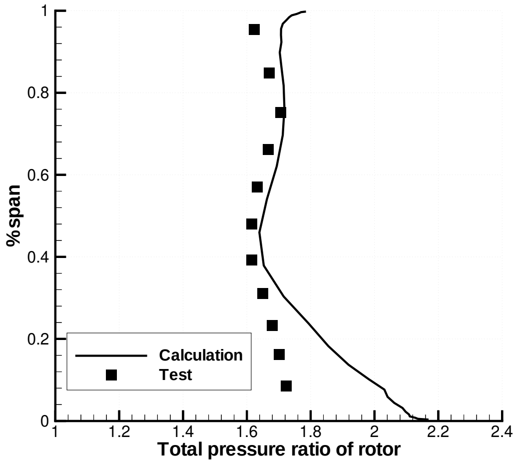

Figure 7: The spanwise variations of total pressure rise at mixing plane

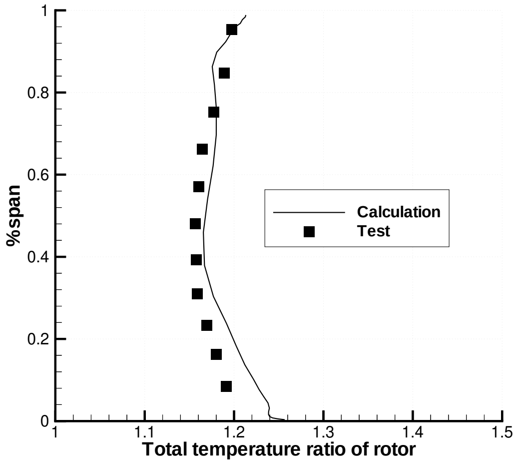

Figure 8: The spanwise variations of total temperature rise at mixing plane

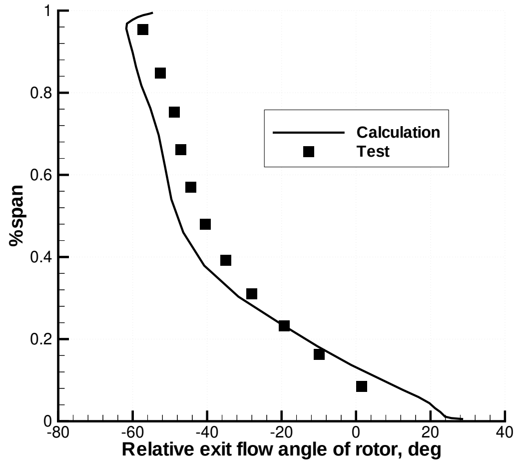

Figure 9: The spanwise variations of relative flow angle at mixing plane

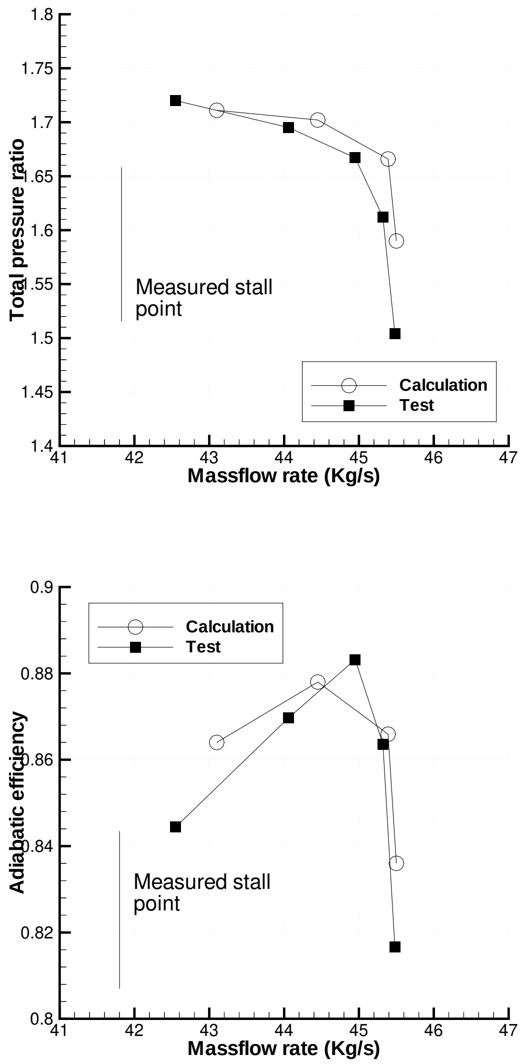

Figure 10: The overall stage performance